A Comparison of Lithology Predictors in Some Thin Bedded Gas Turbidite Reservoirs Using Conventional and Quantum Neural Networks

David K. Potter* and *An H.* Le

Department of Physics, University of Alberta, Edmonton, Alberta, T6G 2E1, Canada

Abstract. Distinguishing between different lithologies is an important component of reservoir characterization. It is particularly important in thin bedded gas turbidite reservoirs, where most of the gas is often located in thin sand layers. If one has core material then identifying the various lithologies can usually be relatively straightforward. However, core retrieval is expensive, so cores are generally only obtained from a small fraction of drilled wells. Thus, lithology profiles need to be estimated from other data such as well logs. The present study compared different neural network approaches to predict lithology in thin bedded gas turbidite reservoirs in two wells in different regions: one in the Nile delta and the other in Miocene sediments in the Polish Carpathian Foredeep. The neural network approaches included (i) conventional single back-propagation neural networks (BPNNs), (ii) modular neural networks (MNNs) that employ a committee of several back-propagation neural networks, and (iii) quantum neural networks (QNNs). The QNNs were tested since some authors in other research areas have proposed that they are potentially better at classification problems than conventional BPNNs, which can sometimes have difficulty distinguishing the boundaries between different classes. The neural networks were trained on combinations of well logs using a genetically focussed methodology, which trains the networks on a short representative interval or genetic unit. This approach is potentially very effective in terms of cost and time. The lithologies predicted by the various approaches were then compared with analysis of the cores for each well. The results for the well in the Nile delta showed that the QNNs overall outperformed the single BPNNs and the MNNs, and were particularly better at predicting the thin sand layers in the test intervals. The results for the well in the Polish Carpathian Foredeep also showed that the QNNs were marginally the best at correctly identifying the sand intervals with depth in the simple **Model 1**, compared to the traditional statistical techniques (involving principal component analysis and discriminant analysis) and the other conventional neural network approaches. QNNs also predicted the highest total number of correct lithologies with depth in the more detailed **Model 2**. In summary, this study indicated the potential of QNNs for improving lithology classification in thin bedded gas turbidite reservoirs. The results also demonstrated that the methodology only requires a short representative interval to train the neural networks in order to deliver good predictions in the much larger test intervals.

1 Introduction

1.1 Traditional Lithology Classification

Lithology classification is usually performed using drill cuttings or core data. Using drill cuttings, however, could lead to incompleteness due to mud swirling, loss of some constituents, or circulation loss. Core data is more useful, but is usually taken only at specific intervals of interest, because it is expensive to obtain, and as a result complete lithological descriptions within wells are not always achieved. Therefore, lithology prediction from wireline logs, which are abundant in most wells, are a potential solution to this problem.

Traditionally, cross plots of two porosity logs (such as neutron-density), or data based on three porosity logs (such as the M and N plot) have been used for lithology determination. Later, computerised methods were also applied, such as the FacioLog (Schlumberger [1]). The Faciolog utilises statistical principal component analysis and cluster analysis to segment the well into clusters where each cluster is related to a different lithofacies. Another statistical method, discriminant analysis, can also be employed to infer lithology from logs. Discriminant analysis takes the original log data and projects the cluster centres as far apart as possible, whilst projecting points from the same cluster closest to each other. Delfiner et al. [2] used the discriminant function (a Bayesian decision rule) to correlate wireline log

* Corresponding author: dkpotter@ualberta.ca

values with a lithofacies database. The method has been tested in several environments and compared with cores and mud log descriptions. Busch et al. [3] also used discriminant analysis to predict lithology with calibration to core data. The approach was applied in a field with a complex mixture of different clastic and carbonate rock types (shale, limestone, siltstone, phosphatic limestone, phosphatic mudrock and sideritic mudrock) with 75% accurate prediction in the test dataset comprising 1,264 samples.

The present study compared various conventional neural network approaches with quantum neural networks to predict lithology in a thin bedded turbidite gas reservoir in a well in the Nile Delta and compared the results with core data. The study also compared standard statistical approaches with conventional and quantum neural networks to predict lithology in a thin bedded turbidite gas reservoir in a well in the Polish Carpathian Foredeep. The results were again compared with core data.

1.2 Lithology Classification from Conventional Neural Networks

Neural networks have been applied by several authors for lithology classification [4-9]. Rogers et al. [4] introduced the first application of feed-forward back-propagation neural networks (BPNNs) for this purpose. In their study, the two neural networks trained on two different theoretical datasets successfully determined the 4 different lithologies (limestone, dolomite, sand, and shale) from well logs. The lithology outcomes from the neural networks in the test dataset agreed well with interpreted lithologies. Three selected wireline logs (bulk density, gamma ray and neutron porosity) were used as input. In the constructed neural network architecture, the number of hidden neurons were 3 and 4 respectively, corresponding to each of the two training datasets, whereas the number of neurons in the output layer was the same, 4, corresponding to the 4 lithofacies to be classified. Wong et al. [5] compared back-propagation neural networks and discriminant analysis. The developed neural network had 3 inputs corresponding to two wireline logs (bulk density and sonic) and the ratio of these logs. A single hidden layer had 4 hidden neurons. The neural network gave a comparable overall outcome to the discriminant analysis approach when predicting 4 different lithofacies (mudstone, sandy mudstone, sand and carbonate cemented beds) in the test dataset comprising 65 core data points. Moreover, the neural network performed better in terms of sand identification with no single misidentification in all 16 sand points.

Note that two approaches can be applied using back propagation neural networks. The first uses a single neural network to predict all the lithologies. This means that the number of output neurons in the output layer is equal to the number of lithologies. The second is the modular neural network (MNN) approach, which employs a committee of many neural networks, and one neural network is trained for predicting only one lithology. The output layer has only one neuron, which predicts a value in the range from 0 to 1. By selecting the highest value from all of the derived output values from each individual network, the final output to the predicted lithology is then assigned. This has been shown to considerably improve the outcomes in several case studies [10,11]. Bhatt and Helle [12] applied modular neural networks to predict 4 depositional facies of the Ness formation, namely channel sand, crevasse, lake and coal in a North Sea oilfield. Initially, the architectures of all neural networks were defined and simulated on synthetic wireline log data based on a model of 3 facies in 17 layers with thicknesses ranging from 3 m to 55 m. One committee, comprising 9 redundantly joined back-propagation neural networks, trained on 9 different training datasets, was used to predict one facies. Five wireline logs (gamma ray, density, neutron porosity, sonic transit time and resistivity) were used as input. The number of hidden neurons was 4. Each training dataset consisted of 60 samples, equally divided for each facies, giving 20 samples per facies. It resulted in a total of 540 training samples. When applied to real data, this committee-modular approach successfully identified 4 facies throughout the field with a misidentification rate of 4.7% in the training well to a maximum of 10% in other wells. The outcomes from the neural network were comparable to the outcomes described from the core data. Therefore, the overall accuracy was quite high. However, the committee was not able to predict the thin coal layers of thickness less than 50 cm, because the layers in the training datasets were at least 3 m. Note that one facies may consist of more than one lithology (crevasse facies consists of fine-grained sand interbedded with clay-rich material).

1.3 Lithology Classification from Quantum Neural Networks (QNNs)

The present paper compares both conventional neural networks and quantum neural networks (QNNs) in conjunction with a Genetic Petrophysics approach, which uses data from a short Representative Genetic Unit (RGU) to train the networks, for lithology prediction from wireline logs in thin bedded turbidite gas reservoirs in (i) the Nile delta, and (ii) Miocene sediments in the Polish Carpathian Foredeep. This is the first time, to our knowledge, that QNNs have been applied to lithology classification, and compared with more traditional approaches in such reservoirs. The main purpose was to find the best way to improve the identification of thin sand bodies within the turbiditic sequences, where most of the gas resides. Previously, thin bed sand identification from wireline logs in these wells had been problematic.

Although conventional feed-forward neural networks trained by back-propagation have been used with success, they can have difficulties recognising the actual lithology in the overlapping areas. The limitation of conventional BPNNs motivated the development of inherently fuzzy feed-forward neural networks, known

as quantum neural networks (QNNs). Purushothaman and Karayiannis [13] first introduced the learning algorithm and architectures of QNNs and claimed that QNNs were able to learn the uncertainty in the sample data. In terms of network architecture, QNNs are still feed-forward neural networks. The major difference between conventional fast forward neural networks (FFNNs) and QNNs is the activation function of the hidden neurons. The hidden neurons of QNNs have multilevel activation functions instead of the conventional sigmoid functions. Each multilevel function is formed as the sum of many sigmoid functions shifted by the quantum intervals. The mathematical formula is as follows:

$$f(x) = \frac{1}{n_s} \sum_{i=1}^{n_s} sgm(\beta_h (x - \theta^i)) \qquad (1)$$

where sgm is the sigmoid function, sgm (x) = $1/(1+e^{-x})$, β_h is a slope factor, θ^i defines the jump position in the transfer function, and n_s is the number of quantum levels in the quantum hidden neurons. If $n_s = 1$ and $\theta^i = 0$, the multilevel activation function becomes the ordinary sigmoid activation function and the QNN becomes a conventional FFNN. For example, the responses of a three-level quantum activation function and a sigmoid activation function are shown in **Figure 1**. The quantum intervals add an additional degree of freedom that can be exploited during the learning process to capture and quantify the structure of the input space [14]. More detail on the QNN learning algorithm is described in [13].

Since the introduction of QNNs, few real-world applications of QNNs have been carried out. Purushothaman and Karayiannis [13] tested QNNs in three different theoretical datasets with positive outcomes. The first was a simple two-class dataset with 16 data points, the second was a three-class hybrid dataset with 60 data points, and the third was a two-class non-convex dataset. Despite the fact that the overall learning time in QNNs was about 50% more than BPNNs the outcomes from QNNs in these training datasets were better than BPNNs. This study established the merit of the QNN architecture for recognising structures in data [13]. Kretzschmar et al. [14] compared the performances of conventional FFNNs and QNNs on two-dimensional speech data. Unlike conventional FFNNs, which produced smooth bell-like surfaces for each class, QNNs quantized certain regions of the input space by creating staircase-like surfaces for each class. Therefore, they concluded that QNNs are capable of representing and quantifying the uncertainty inherent in the training data. It was also shown that simple post-processing of the QNN outputs made QNNs an attractive alternative to conventional FFNNs for pattern classification applications [14].

Lithology classification from wireline logs is, to a certain extent, a fuzzy classification. Conventional wireline log responses may not always identify thin beds. The present study was partly designed to see if QNNs could improve lithology classification in turbidite reservoirs where thin sand beds exist.

2 Datasets and Methods

2.1 Nile Delta Datasets and Neural Network Lithology Predictors

In the Nile Delta dataset, wireline log data from a 40 m interval and core photos from the lower 29 m of this interval were provided. The high resolution wireline log data was recorded at about every 9 cm depth. Since no depth shift was provided by the company, high-resolution probe magnetic susceptibility measurements on the slabbed core [15] were used as a tool to deduce the depth shift. A comparison between the magnetic susceptibility measurements and the wireline gamma ray log allowed an approximate depth shift to be made. A Representative Genetic Unit (RGU) was selected from the slabbed core and its wireline log signature in order to train the various neural network predictors. This 4 m long RGU consisted of representative lithologies seen in the entire cored interval of the well. It included a Bouma sequence comprising a basal graded fining upwards sand overlain by a thin interval of plane laminations, cross laminations and then shale. The RGU also comprised two types of sand in the turbidite sequences: a relatively clean sand, and a greenish sand containing some clay (including glauconite). The number of training data points in the RGU was 46 compared to 328 in the entire cored interval.

Three main Genetically Focussed Neural Network (GFNN) training datasets were constructed based on the encoded lithology according to the core description in conjunction with input wireline logs as follows:

(i) The first dataset used three key wireline logs (gamma ray, bulk density and sonic transit time) resulting in 3 inputs to the neural network,

(ii) The second dataset added an extra porosity log (neutron porosity) to the above combination of three key wireline logs, resulting in 4 inputs to the neural network.

(iii) The third dataset added a high-resolution resistivity log, the micro laterolog (MLL), to the above combination of three key wireline logs (instead of neutron porosity), resulting in 4 inputs to the neural network.

All the neural network simulations were carried out using the Linux-based version of the Stuttgart Neural Network Simulator (SNNS). For the first training dataset, three neural network approaches were carried out as follows:

BP3-2. Firstly, a back-propagation learning algorithm was used to train a feed-forward neural network to predict 2 lithologies: sand and shale. The hidden layer contained 4 hidden neurons and the output layer contained two output neurons: sand and shale. Therefore BP3-2 directly outputs either sand or shale (the numbers 3-2 refer to the number of inputs and outputs respectively).

MNN3-2. Secondly, the modular approach was employed to predict the lithology. The committee

MNN3-2 consisted of two neural networks, BP3-Sa and BP3-Sh, which were trained separately using a back-propagation algorithm to predict sand or shale respectively. The encoded lithology was represented as 0 or 1 depending on the neural network. For BP3-Sa the encoded value was 1 for sand and 0 for shale. For BP3-Sh the encoded value was 0 for sand and 1 for shale. The final output of lithology was selected by comparing the output from the two component networks in the committee MMN3-2.

QNN3-2. Thirdly, a quantum neural network was trained to directly predict lithology. The hidden layer contained 4 hidden neurons with 3 quantum levels (i.e. the quantum activation function had 3 quantum levels) and the output layer contained two output neurons: sand and shale. Thus QNN3-2 directly outputs 2 types of lithology: sand or shale.

For the second and the third datasets, three similar modified neural network approaches were carried out as follows:

BP4-2 (I) and (II). Again a back-propagation learning algorithm was used to train a feed-forward neural network to predict 2 lithologies: sand and shale. The hidden layer this time contained 5 hidden neurons and the output layer contained two output neurons: sand and shale. "I" denotes the second training dataset and "II" denotes the third training dataset.

MNN4-2 (I) and (II). The modular committee MNN4-2 consisted of two neural networks, BP4-Sa and BP4-Sh, which were separately trained using a back-propagation learning algorithm to predict sand and shale. The final output of lithology was selected by comparing the output from the two component networks BP4-Sa and BP4-Sh in the committee MMN4-2.

QNN4-2 (I) and (II). Quantum neural networks were again trained to directly predict lithology. This QNN4-2 used the same wireline logs and lithological data as for BP4-2. The hidden layer this time contained 5 hidden neurons with 3 quantum levels, and the output layer contained two output neurons: sand and shale. Thus QNN4-2 also directly output 2 types of lithology: sand or shale.

2.2 Polish Carpathian Foredeep Datasets, Statistical Predictors and Neural Network Lithology Predictors

The prediction of sandstone beds with depth using wireline logs by different approaches in the Miocene sediments from the Polish Carpathian Foredeep has previously been problematic. This is due to several reasons. Firstly, the thin interbedded sand and shale nature of these turbidite deposits, as well as the absence of thick sand (most sand beds are less than 1 m in thickness). Secondly, the lack of any high-resolution logs other than the micro-spherically focussed log (MSFL), and the lower sampling rate of wireline logs measurement (at 25 cm) within the limited log suite that is available. Partly because of that, the MSFL did not exhibit any higher resolution detail than other resistivity logs: deep induction (ILD), medium induction (ILM), deep laterolog (LLD), and shallow laterolog (LLS).

The data available for the well in the Polish Carpathian Foredeep for the present study comprised wireline log data in the depth interval from XX45–XX98.75 m. This interval was cored in the sections XX45–XX55.5 m and XX57–XX98.75 m. All conventional wireline logs (gamma ray, spectral gamma ray, resistivity, neutron porosity, sonic transit time and bulk density) were available. The wireline log data was recorded at every 25 cm depth. Detailed lithological description of the core in these cored sections was also available.

Initially, the logs were depth matched as closely as possible to the core data. This refined depth matching was conducted by constructing a synthetic lithology curve from core data. The synthetic lithology curve in sand content percentages was calculated using 0.5 m vertical resolution and 0.25 m steps, which were close to the gamma ray resolution and measurement steps, so it was then matched to the gamma ray log.

The 19 m interval from XX71–XX90 m was selected as the training interval, as it seemed representative of the range of lithologies present in the well. A relatively large coarsening upward sequence was observed throughout this interval obtained from the core description. The basal section consisted of a thick shale layer of about 6 m, overlain by 6 m of thick shale interbedded with thin sand layers having less than 40% of sand content. The top section contained 7 m of shale and sand interbedded with more than 50% of sand content according to the core analysis.

Principal component (PC) analysis and discriminant analysis (DA) were carried out in this training interval for lithology prediction throughout this well. The outcomes from these statistical approaches have been compared to the outcomes from the neural network approaches in this study.

The training datasets for the neural network simulations were then constructed based on two models as detailed bellow. The number of wireline logs used as input in the neural network simulations was 3, namely gamma ray, sonic transit time, and neutron porosity logs (GR, DT and NPHI). The reason for choosing these particular three logs is twofold. Firstly, previous studies suggested that the gamma ray combined with one or two porosity logs gave good prediction of petrophysical parameters in sand-shale lithologies [16,17]. Secondly, some initial results of statistical approaches suggested that these were important logs for differentiating the lithologies. Sand content in percentage (%) derived from core analysis was used to classify lithologies based on the criteria of two models as follows:

Model 1:

Sand: if the sand content is more than 50%.
Shale: if the sand content is less than 50%.

Model 2:

Sand: if the sand content is more than 80% then it is sand.
Shaly sand: if the sand content is from 50 % to 80%.
Sandy shale: if the sand content is from 20 % to 50%.
Shale: if the sand content is less than 20%.

Sand content (%) was estimated from the core, and then converted to lithology according to the two models. The results were then compared with the predictions from the statistical and neural network approaches. All neural network simulations were carried out again using the Linux-based version of the Stuttgart Neural Network Simulator. The three main neural network approaches in this study were carried out as follows:

NN3-1. Firstly, a conventional feed forward neural network was trained to predict sand content in volume percentage. The TACOMA learning algorithm [18] was applied to train the network. The training data consisted of 3 wireline logs (GR, DT and NPHI), along with the core derived value of sand content in the training interval. The trained neural network produced one output: sand content. The predicted sand content was consequently used to characterise the lithology according to the criteria in **Model 1** and **Model 2**.

NN3-2 and NN3-4. Secondly, conventional feed forward neural networks were trained to directly predict lithology. The TACOMA learning algorithm was again applied to train the network. In these cases, the training data consisted of encoded lithology (derived from the core data in the training interval according to the two models), along with the 3 key wireline log inputs (GR, NPHI and DT). For NN3-2, which corresponded to **Model 1**, the lithology consisted simply of 2 types (sand and shale), so the output layer had two output neurons for the two lithologies: sand and shale. For NN3-4, which corresponded to **Model 2**, the lithology now consisted of 4 types (sand, shaly sand, sandy shale and shale), so the output layer had 4 output neurons for these 4 lithologies.

QNN3-2 and QNN3-4. Thirdly, quantum neural networks were trained to directly predict lithology. QNN3-2 and QNN3-4 used the same wireline logs and lithological data as for NN3-2 and NN3-4. The difference was the hidden layer in the quantum neural networks, which contained 4 hidden neurons with 3 quantum levels. Thus the QNN3-2 output consisted of 2 types of lithology for **Model 1**, whereas the QNN3-4 output consisted 4 types of lithology for **Model 2**.

3 Results and Discussion

3.1 Results and Discussion for the Nile Delta well

Table 1 (a) summarizes the results for the number of correctly predicted lithologies at the correct depths for all the approaches in the test interval. The outcomes of the lithology predictions with depth for the first dataset using three key wireline logs (DT, GR and RHOB) as input are shown in **Figure 2**. The results showed that the neural network lithology predictions agreed quite well with the core lithology. The predictors gave 183 to 200 correct values for the lithology elements out of 282, i.e. from 65% to 71% in the test interval.

The predictions normally improved when moving from conventional back-propagation neural networks to modular neural networks and then to quantum neural networks for all three training datasets, except that MNN4-2 and QNN4-2 gave almost identical results. When using 3 wireline logs (first training dataset), the total number of correct values increased from 185 (BP3-2 predictor) to 187 (MNN3-2 predictor) to 198 (QNN3-2 predictor). When using 4 wireline logs (second training dataset), the total number of correct predicted values increased from 190 (BP4-2(I) predictor) to 200 (both MNN4-2(I) and QNN4-2(I) predictors). When the high-resolution resistivity log MLL was used (third training dataset), the total number of correctly predicted values increased from 183 (BP4-2(II) predictor) to 187 (MNN4-2(II) predictor) and then 186 (QNN4-2(II) predictor).

Note that QNN3-2 was the best at sand identification, giving 65 correct values out of a total of 111. This is particularly important in this well, since most of the gas is in the thin sand intervals. QNN4-2(I) was the best shale identifier, giving 152 correct values out of a total of 171.

The differences between the core lithology and the predictions with depth by the various neural network approaches employed could be due to slight inaccuracies in the depth matching between the core and log data in the highly heterogeneous test interval. Therefore, to assess the possible influence of depth shifting, the total numbers of predicted lithology elements from each neural network predictor were also calculated. **Table 1 (b)** summarises the results for the test interval. This shows that the total amount of sand was better predicted by all predictors (compared to the results of **Table 1 (a)**). The best outcomes were from the QNN3-2 predictor, which predicted 100 sand elements and 182 shale elements, compared to the core values of 111 sand elements and 171 shale elements. These results are better than those derived from the conventional back-propagation neural networks (although BP4-2(II) was very close), and suggest that quantum neural networks can provide significantly better estimates of net sand to gross ratio in thin interbedded turbidite reservoirs. Note that QNN3-2 correctly identified the sand layers at depths XX35.2–XX35.8 m and XX42.03–XX42.41 m, whereas all other predictors failed to identify them. Moreover, QNN3-2 was also good at identification of thin sand layers, for example the 9 cm sand layer at depth XX56.55 m, which all other predictors missed.

3.2 Results and Discussion for the Polish Carpathian Foredeep well

Table 2 (a) summarises the results for the number of correctly predicted lithologies at the correct depths for **Model 1** for all the approaches in the test intervals. The outcomes of the lithology predictions with depth for all approaches for **Model 1** are shown in **Figure 3**. All methods gave reasonable outcomes in the test intervals with results ranging from 60%–73% of the correct values. Discriminant analysis on the principal components gave the best results scoring 98 correct lithologies out of a total of 134 and the neural net approach QNN3-2 gave 96 correct results. The QNN3-2 was again best at identifying the sand, whilst the

discriminant analysis on principal components was marginally best at identifying the shale.

The differences between the core lithology and the predictions with depth by the various neural network approaches employed could be due to one or more of the following reasons:

1. Slight inaccuracies in the depth matching between core and log data.
2. The selected training interval may have not been completely representative of the overall well interval.
3. The wireline log resolution is lower (at 25 cm per reading, compared to the high resolution logs of 9 cm per reading for the Nile Delta well) whereas the core description was continuous at high resolution.

In order to assess the possible influence of slight inaccuracies in depth matching on the results, the total numbers of each lithology from each method were compared to the totals given by the core data (i.e., the values ignored whether the lithologies were predicted in the correct positions with depth compared to the core). These values are given in **Table 2 (b)** for the test intervals for **Model 1**. The total values for sand and shale by each method are very close to those given by the core data, suggesting that slight inaccuracies in depth matching is a likely explanation for the differences with depth between the predicted lithologies and those indicated by the core description. The results suggest that the net to gross ratio is well predicted even if the exact location of the sand beds are less well predicted.

Table 3 (a) summarises the results for the number of correctly predicted lithologies at the correct depths for **Model 2** for all the approaches in the test intervals. The outcomes of the lithology predictions with depth for all approaches for **Model 2** are shown in **Figure 4**. All methods gave relatively good outcomes for shale in the test intervals, with results ranging from 68–74% of the correct values. However, for all methods the outcomes were significantly lower for the remaining 3 lithologies (sand, shaly sand, and sandy shale). The QNN3-4 and NN3-4 approaches gave marginally better results in the test intervals. The reason the neural net approaches gave slightly better results than the statistical methods in the test intervals may be partly because the neural network matched the actual values better within the training interval.

Table 3 (b) for **Model 2** showed that the total amount of sand in the test intervals is again generally better predicted than the number of correct sand values with depth given in **Table 3 (a)**, particularly for the NN3-4 approach. However, the total amount of shale is over-predicted, whilst the shaly sand and sandy shale are generally under-predicted.

4 Conclusions

The following conclusions can be drawn:

4.1 General

1. QNNs have been successfully applied to lithology classification in thin bedded turbidites, we think for the first time, suggesting this could be a promising approach for other heterogeneous depositional environments.
2. Identifying thin sand bodies in turbidite sequences using conventional statistical approaches (principal component analysis and discriminant analysis) and wireline log data has often been problematic. However, neural networks trained on representative data have demonstrated good predictions verified by core in this study. In general, QNNs provided better outcomes compared to conventional feed-forward BPNNs and MNNs, especially in the task of sand body identification.

4.2 Nile Delta well

3. The QNN predictors were particularly better at predicting the sand, including thin sand intervals, compared to the other neural net approaches. This is especially important in this well where the sand intervals contain most of the gas.
4. The use of three key wireline logs (GR, DT, and RHOB) as input for the QNN predictor was better than two other cases that used an additional wireline log.
4. The total number of each predicted lithology (irrespective of whether the predictions were correctly predicted at the exact depth) gave better results than the total number of correct predictions with depth. This suggests that predictions with depth in the test intervals are likely to better match the actual lithology from core data with improved depth shifting of the high resolution log and core data. One approach could be to use high-resolution measurements (such as probe magnetic susceptibility [15]) to improve the depth shifting, as was done and verified in the training dataset.
5. Integrating the Genetic Petrophysics approach, utilizing a small Representative Genetic Unit (RGU) for training with QNNs, is potentially very cost-effective, and should be especially useful in other studies where limited data is available.

4.3 Polish Carpathian Foredeep well

6. Both the statistical and neural network techniques gave good predictions of the total amounts of each lithological element, whereas the exact predictions with depth were less well predicted. Moreover, the predictions for the simple **Model 1** were better than for the slightly more detailed **Model 2**. These results suggested that slight inaccuracies in depth matching, which was difficult due to the poorer resolution of the logs, was a likely explanation. Therefore good depth matching of the logs to the core data is necessary for accurately predicting the variations with depth.

D. K. P. thanks the Natural Sciences and Engineering Research Council of Canada (NSERC) for a Discovery Grant.

5 List of Abbreviations

BPNN	Back-Propagation Neural Network
DT	Delta T (Acoustic Transit Time)
FFNN	Feed-Forward Neural Network
GFNN	Genetically Focused Neural Network

GR	Gamma Ray
ILD	Deep Induction log
ILM	Medium Induction log
LLD	Deep Laterolog
LLS	Shallow Laterolog
MLL	Micro Laterolog
MNN	Modular Neural Network
MSFL	Micro-Spherically Focused Log
NPHI	Neutron Porosity
QNN	Quantum Neural Network
RHOB	Bulk Density
RGU	Representative Genetic Unit
SNNS	Stuttgart Neural Network
TACOMA	Task Decomposition by Correlation Measures

6 References

1. Schlumberger. Log Interpretation Principles/ Applications (1989).
2. P. Delfiner, O. Peyret, and O. Serra. Automatic Determination of Lithofacies from Well Logs. SPE Formation Evaluation, **2**, 303-310 (1987).
3. J. M. Busch, W. G. Fortney, and L. N. Berry. Determination of Lithology from Well Logs by Statistical Analysis. SPE 14301 (1987).
4. S. J. Rogers, H. C. Chen, D. C. Kopaska-Merkel, and J. H. Fang. Determination of Lithology from Well Logs using a Neural Network. AAPG Bulletin, **76**(5), 731-739 (1992).
5. P. M. Wong, F. X. Jian, and I. J. Taggart. A Critical Comparison of Neural Networks and Discriminant Analysis in Lithofacies, Porosity and Permeability Predictions. Journal of Petroleum Geology, **18**, 19 – 206 (1995).
6. G. Wadge, D. Benaouda, G. Ferrier, R. B. Whitmarsh, R. G. Rothwell, and C. Macleod, C., 1998. Lithological Classification Within ODP Holes using Neural Networks Trained from Integrated Core-Log Data. In: P. K. Harvey and M. A. Lovell, eds., *Core-Log Integration*. Geological Society Special Publication, **136**, 129-140 (1998).
7. M. M. Saggaf and E. L. Nebrija. Estimation of Lithologies and Depositional Facies from Wire-Line Logs. AAPG Bulletin, **84**(10), 1633-1646 (2000).
8. H. Chang, D. C. Kopaska, H. Chen, and R. S. Rurrans. Lithofacies Identification using Multiple Adaptive Resonance Theory Neural Networks and Group Decision Expert System. Computer and Geoscience, **26**, 591-601 (2000).
9. A. Bhatt and H. B. Helle. Committee Neural Networks for Porosity and Permeability Prediction from Well Logs. Geophysical Prospecting, **50**, 645-660 (2002a).
10. R. Anand, K. Mehrotra, C. K.. Mohan, and S. Ranka. Efficient Classification for Multi-Class Problems using Modular Neural Networks. IEEE Transactions on Neural Networks, **6**, 117–124 (1995).
11. H. B. Helle and A. Bhatt. Fluid Saturation from Well Logs using Committee Neural Networks. Petroleum Geoscience, **8**, 109-118 (2002).
12. A Bhatt and H. B. Helle. Determination of Facies from Well Logs using Modular Neural Networks. Petroleum Geoscience, **8**, 217-228 (2002b).
13. G. Purushothaman and N. B. Karayiannis. Quantum Neural Networks (QNN's): Inherently Fuzzy Feedforward Neural Networks. IEEE Transactions on Neural Networks, **8**(3), 679-693 (1997).
14. R. Kretzschmar, R. Bueler, N. B. Karayiannis, and F. Eggimann. Quantum Neural Networks versus Conventional Feed Forward Neural Networks: An Experimental Study. *2000 IEEE International Workshop on Neural Networks for Signal Processing (NNSP'2000)*, 328-337 (2000).
15. T. H. To and D. K. Potter. Comparison of High-Resolution Probe Magnetics, X-ray Fluorescence and Permeability on Core with Borehole Spectral Gamma Ray and Spontaneous Potential in an Oil Sand Well. *Proceedings of the 34th International Symposium of the Society of Core Analysts (online symposium 13-16 September)*, Paper SCA2021-035, 12 pages (2021).
16. A. H. Le and D. K. Potter. Genetically Focused Neural Nets for Permeability Prediction from Wireline Logs. *European Association of Geoscientists and Engineers 65th Conference, Stavanger, 2-5 June*, Paper F28 (2003).
17. D. K. Potter, A. H. Le, P. W. M. Corbett, C. McCann, S. Assefa, T. Astin, J. Sothcott, B. Bennett, S. Larter, and A. Lager. Genetic Petrophysics Approach to Core Analysis – Application to Shoreface Sandstone Reservoirs. *Proceedings of the 17th International Symposium of the Society of Core Analysts*, Paper SCA2003-35, 12 pages, Pau, France (2003).
18. J. M. Lange, H. M. Voigt, and D. Wolf. Task Decomposition and Correlations in Growing Artificial Neural Networks. *Proceedings of IC on ANN*, 753-758 (1994).

Table 1. (a) Comparisons of the number of correctly predicted lithological elements at the correct depths from the various neural network predictors, along with the core values, in the Test Interval (XX35–XX60 m) of the cored section of the well in the Nile Delta. **(b)** Comparisons of the number of predicted lithological elements in the same Test Interval, irrespective of whether those lithological elements were predicted at the correct depths.
*Indicates the best sand predictor in each case.

(a)

Lithology	Core	BP3-2	MNN3-2	QNN3-2	BP4-2		MNN4-2		QNN4-2	
					I	II	I	II	I	II
Sand	111	36	42	65*	48	54	51	53	48	43
Shale	171	149	145	133	142	129	146	134	152	143
Total	282	185	187	198	190	183	200	187	200	186

(b)

Lithology	Core	BP3-2	MNN3-2	QNN3-2	BP4-2		MNN4-2		QNN4-2	
					I	II	I	II	I	II
Sand	111	58	71	100*	73	98	76	90	77	71
Shale	171	224	221	182	209	184	206	192	205	211
Total	282	282	282	282	282	282	282	282	282	282

Table 2. (a) Comparisons of the number of correctly predicted lithological elements at the correct depths from the various statistical and neural network predictors, along with the core values, in the Test Intervals (XX45–XX70 m and XX90–X100 m) of the cored section of the well in the Polish Carpathian Foredeep for **Model 1**. DA = Discriminant Analysis, and PC = Principal Components. **(b)** Comparisons of the number of predicted lithological elements in the same Test Interval, irrespective of whether those lithological elements were predicted at the correct depths.
*Indicates the best sand predictor(s) in each case.

(a)

Lithology	Core	DA on Raw Data	DA on PC	NN3-1	NN3-2	QNN3-2
Sand	53	33	33	28	22	34*
Shale	81	56	65	56	58	62
Total	134	89	98	84	80	96

(b)

Lithology	Core	DA on Raw Data	DA on PC	NN3-1	NN3-2	QNN3-2
Sand	53	58	51	53*	45	53*
Shale	81	76	83	81	89	81
Total	134	134	134	134	134	134

Table 3. (a) Comparisons of the number of correctly predicted lithological elements at the correct depths from the various statistical and neural network predictors (*indicates the best overall predictor), along with the core values, in the Test Intervals (XX45–XX70 m and XX90–X100 m) of the cored section of the well in the Polish Carpathian Foredeep for **Model 2**. DA = Discriminant Analysis, and PC = Principal Components. **(b)** Comparisons of the number of predicted lithological elements in the same Test Interval, irrespective of whether those lithological elements were predicted at the correct depths.

(a)

Lithology	Core	DA on Raw Data	DA on PC	NN3-1	NN3-4	QNN3-4
Sand	17	2	3	6	2	5
Shaly Sand	36	18	8	7	7	6
Sandy Shale	50	5	12	12	18	22
Shale	31	21	22	21	23	21
Total	134	46	45	46	50	54*

(b)

Lithology	Core	DA on Raw Data	DA on PC	NN3-1	NN3-4	QNN3-4
Sand	17	5	24	33	17	30
Shaly Sand	36	51	30	20	21	20
Sandy Shale	50	15	24	26	37	41
Shale	31	63	56	55	59	43
Total	134	134	134	134	134	134

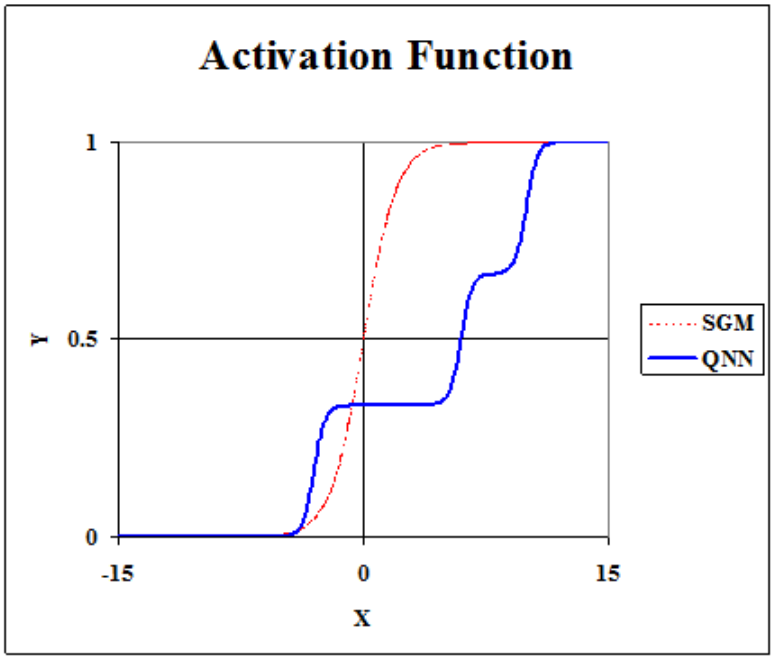

Fig. 1. The responses of a three-level quantum activation function (QNN) and sigmoid activation function (SGM).

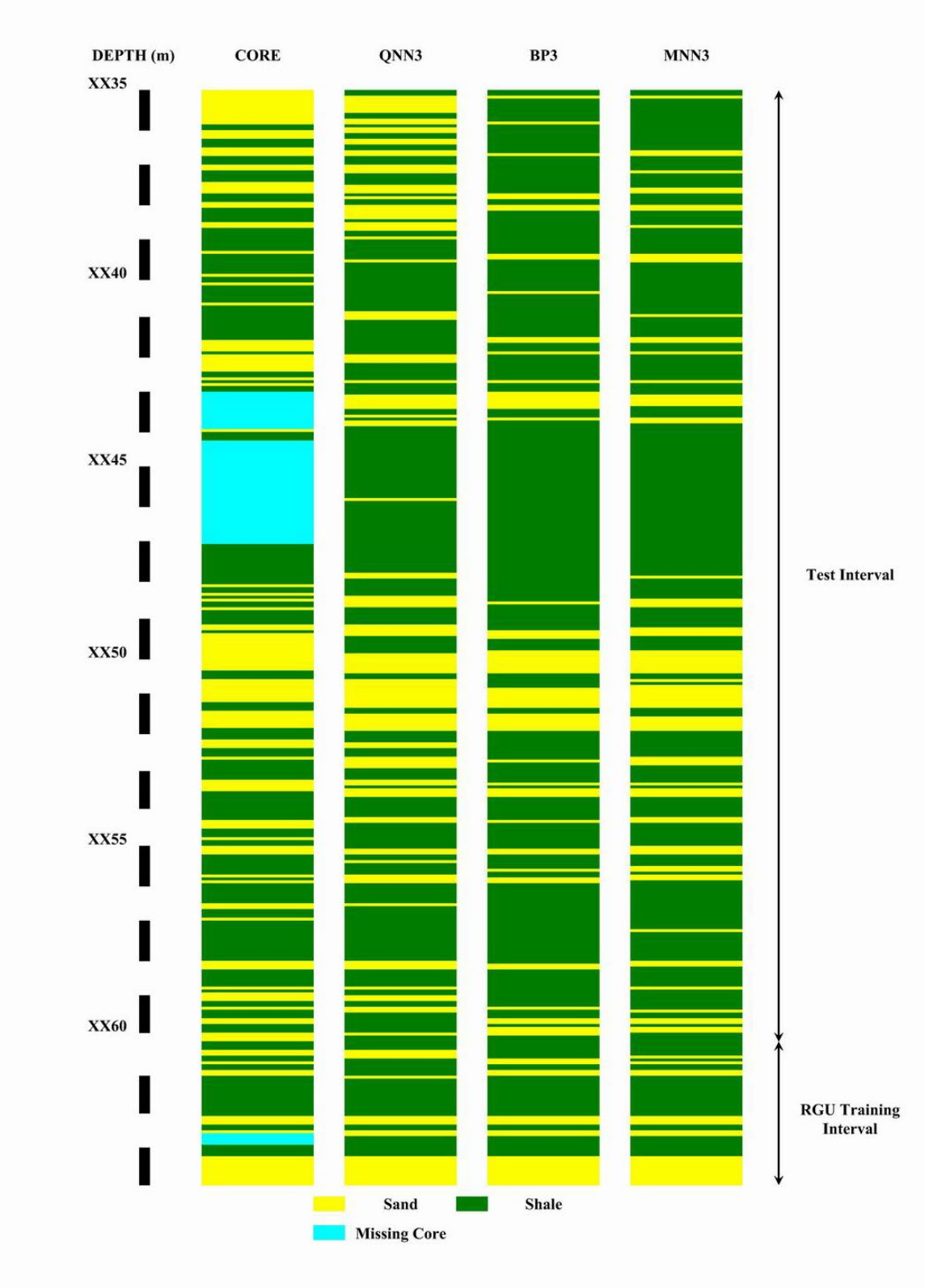

Fig. 2. Comparisons of the lithology predictions with depth from neural network predictors for the first training dataset using 3 key wireline logs (DT, GR, RHOB), along with the core derived lithology, in the training and test intervals of the well in the Nile Delta.

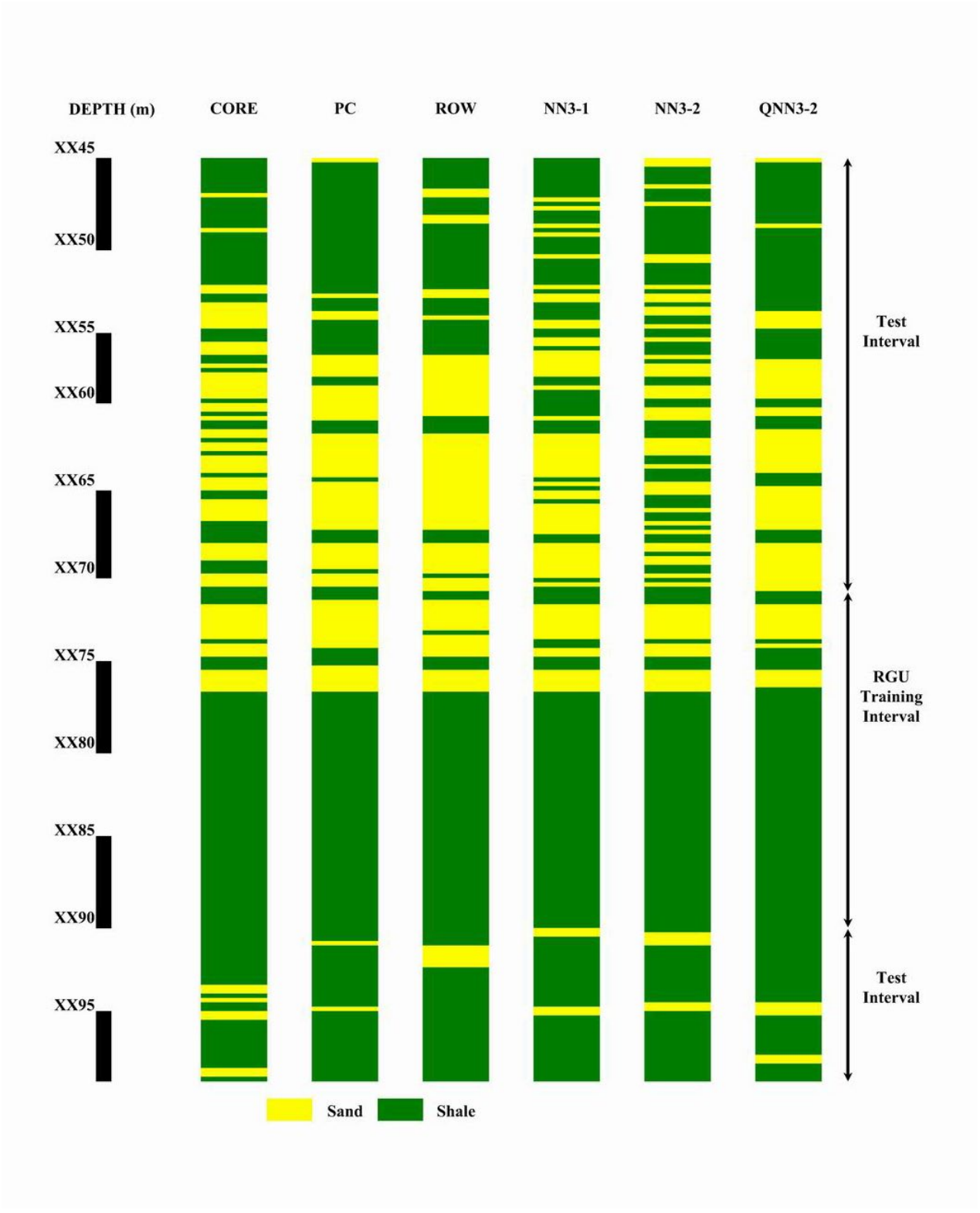

Fig. 3. Comparisons of the lithology predictions with depth from statistical and neural network predictors, along with the core derived lithology, in the training and test intervals of the well in the Polish Carpathian Foredeep for **Model 1**. PC refers to discriminant analysis on the principal components, and ROW refers to discriminant analysis on the raw data output from the well.

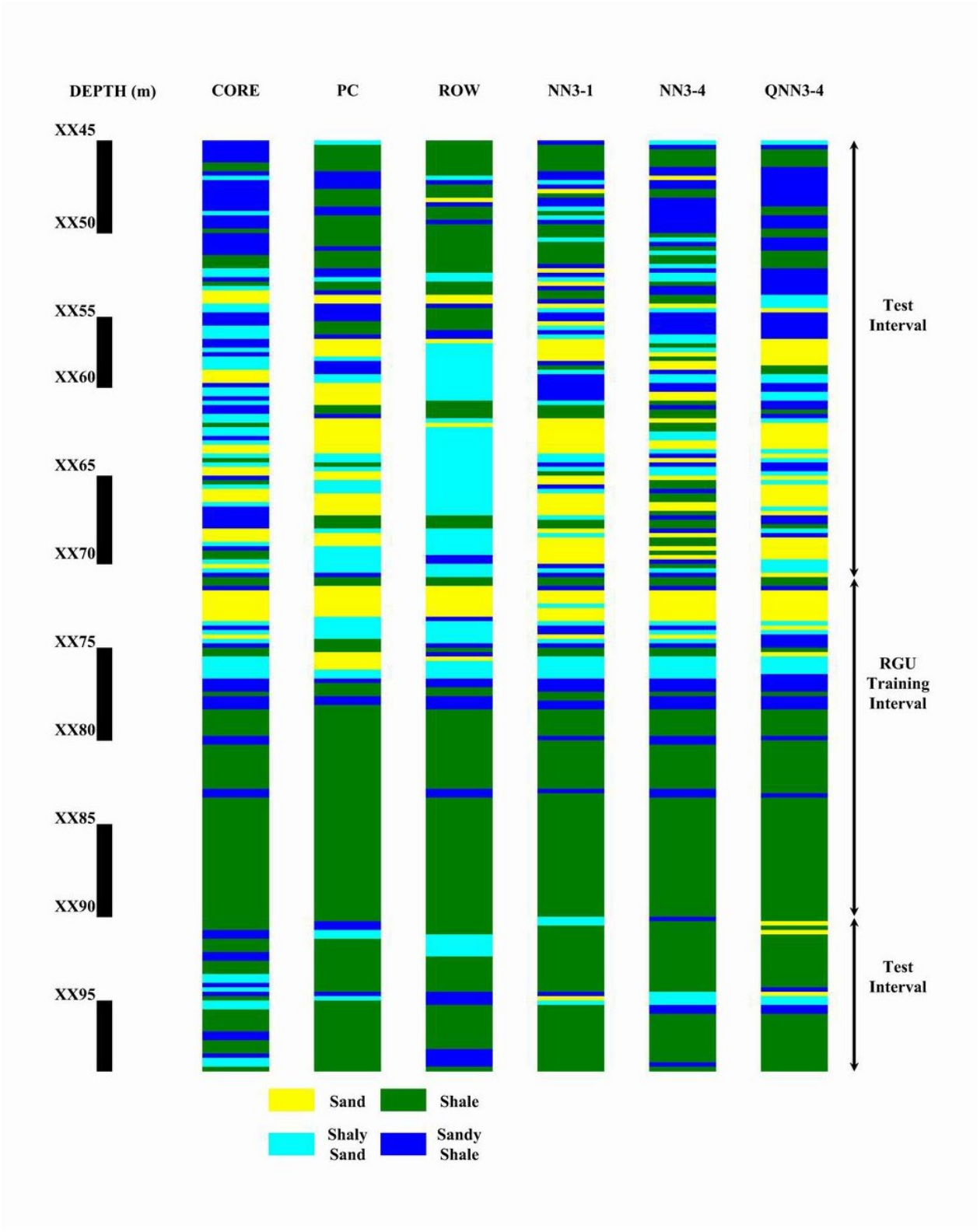

Fig. 4. Comparisons of the lithology predictions with depth from statistical and neural network predictors, along with the core derived lithology, in the training and test intervals of the well in the Polish Carpathian Foredeep for **Model 2**. PC refers to discriminant analysis on the principal components, and ROW refers to discriminant analysis on the raw data output from the well.